ARTICLE

Cupric-superoxide complex that induces a catalytic aldol reaction-type C–C bond formation

Tsukasa Abe [1], Yuta Hori[2], Yoshihito Shiota [2], Takehiro Ohta [3], Yuma Morimoto[1], Hideki Sugimoto[1], Takashi Ogura[3], Kazunari Yoshizawa[2] & Shinobu Itoh[1]

Much recent attention has been focused on the structure and reactivity of transition-metal superoxide complexes, among which mononuclear copper(II)-superoxide complexes are recognized as key reactive intermediates in many biological and abiological dioxygen-activation processes. So far, several types of copper(II)-superoxide complexes have been developed and their electrophilic reactivity has been explored in C–H and O–H bond activation reactions. Here we demonstrate that a mononuclear copper(II)-(end-on)superoxide complex supported by a N-[(2-pyridyl)methyl]-1,5-diazacyclooctane tridentate ligand can induce catalytic C–C bond formation reaction between carbonyl compounds (substrate) and the solvent molecule (acetone), giving β-hydroxy-ketones (aldol). Kinetic and spectroscopic studies at low temperature as well as DFT calculation studies support a nucleophilic reactivity of the superoxide species toward the carbonyl compounds, providing new insights into the reactivity of transition-metal superoxide species not only in biological oxidation reactions but also in synthetic organic chemistry.

[1] Department of Material and Life Science, Division of Advanced Science and Biotechnology, Graduate School of Engineering, Osaka University, 2-1 Yamadaoka, Suita, Osaka 565-0871, Japan. [2] Institute for Materials Chemistry and Engineering and IRCCS, Kyushu University, 744 Motooka, Nishi-ku, Fukuoka 819-0395, Japan. [3] Picobiology Institute, Graduate School of Life Science, University of Hyogo, RSC-UH LP Center, Koto 1-1-1, Sayo-cho, Sayo-gun, Hyogo 679-5148, Japan. Correspondence and requests for materials should be addressed to K.Y. (email: kazunari@ms.ifoc.kyushu-u.ac.jp) or to S.I. (email: shinobu@mls.eng.osaka-u.ac.jp)

Dioxygen activation by low-valent transition metal complexes is involved in many biological and abiological oxidation reactions, where the formation of superoxide complex is a fundamental common process.[1,2] Such superoxide complexes can act as a direct oxidant or a precursor of other types of reactive intermediates for oxidative transformation reactions.[3–11] In copper case, some end-on and side-on superoxide copper(II) complexes have been characterized and their reactivity has been examined mostly in hydrogen atom abstraction (HAA) from C–H and O–H bonds of organic compounds.[12–22] In general, copper(II)-(end-on)superoxide complexes supported by neutral tridentate or tetradentate nitrogen-based ligands exhibit electrophilic reactivity in such HAA reactions.[16,18,23,24] On the other hand, McDonald and coworkers investigated the reaction of copper(II)-(end-on)superoxide complex and some carbonyl compounds by using Tolman's superoxide copper(II) complex supported by a deprotonated diamide-pyridine (dianionic) ligand.[15,25] The superoxide complex exhibits formally nucleophilic reactivity toward the carbonyl compounds to induce the oxidative transformation reactions such as conversion of acid chlorides to carboxylic acids and Baeyer–Villiger oxidation and oxidative deformylation of aldehydes.[25] They proposed that nucleophilic addition of the distal oxygen of superoxide moiety to the carbonyl carbon of the substrates is the key step in such reactions based on the reactivity study of the series of substrates.[25] They suggested that such a nucleophilic reactivity is due to strong electron donor ability of the deprotonated dianionic supporting ligand.[25]

As our continuing research efforts in copper(I)-dioxygen chemistry, we have also developed a mononuclear copper(II)-(end-on)superoxide complex 2 using an N_3-tridentate ligand L^{Pye} consisting of an eight-membered cyclic diamine with a 2-(2-pyridyl)ethyl sidearm (–CH$_2$CH$_2$Py; Py = 2-pyridyl) (Fig. 1).[14,23] Our superoxide complex is a unique example that induces an benzylic C–H bond hydroxylation reaction, mimicking the reactivity of copper monooxygenases such as dopamine β-monooxygenases and peptidylglycine α-hydroxylating monooxygenases.[14,23] Detailed mechanistic studies have indicated that the superoxide complex 2 exhibits an electrophilic reactivity in the C–H bond hydroxylation reaction.

In this study, we examine the reactivity of another mononuclear (end-on)superoxide complex 1 generated by using a similar N_3-tridentate ligand L^{Pym}, which has a shorter pyridylmethyl sidearm (–CH$_2$Py) instead of the pyridylethyl one (–CH$_2$CH$_2$Py) in L^{Pye} (Fig. 1). In this case, superoxide complex 1 exhibits completely different reactivity from that of 2 to induce catalytic C–C bond formation between carbonyl compounds (substrates) and the solvent molecule (acetone), giving β-hydroxy-ketones (aldol). Such a C–C bond formation reaction does not occur at all with superoxide complex 2. Thus, a subtle ligand modification (–CH$_2$CH$_2$Py to –CH$_2$Py) greatly impacts the reactivity of the generated copper(II)-(end-on)superoxide complexes. Kinetic and spectroscopic studies at a low temperature
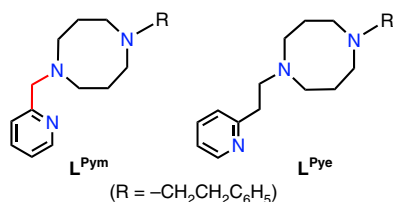
(e.g. –95 °C) indicate that nucleophilic addition of the superoxide species to the carbonyl carbon of the substrate is involved as an initial step of the C–C bond formation reaction. Mechanistic details are further evaluated by DFT (density functional theory) calculation studies to provide new insights into the reactivity of the transition metal superoxide species. So far, a number of copper-catalyzed aldol reactions have been reported,[26] but the role of copper has been simply considered as a Lewis acid catalyst. The present study demonstrates interesting synergistic effects of the superoxide ligand and Lewis acidic metal center for the catalytic C–C bond formation reaction, thus providing a new insight into the role of copper catalyst in synthetic organic chemistry.

Results

Synthesis and characterization of copper complexes. The precursor copper(I) complex of L^{Pym} was prepared by mixing an equimolar amount of the ligand and [Cu^I(CH$_3$CN)$_4$](PF$_6$) in THF under anaerobic conditions (in a glovebox). Single crystals of the copper(I) complex suitable for X-ray crystallographic analysis were obtained as a BPh$_4^-$ salt, [Cu^I(L^{Pym})](BPh$_4$), by treating the generated copper(I) complex with NaBPh$_4$ (for synthetic procedures and characterization, see Supplementary Methods and Supplementary Fig. 1 and Supplementary Tables 1 and 2). The copper(I) complex exhibits a distorted three-coordinate T-shape structure involving the three nitrogen atoms of the ligand, which is stabilized by an intramolecular d–π interaction between the copper(I) ion and the ipso-carbon atom of the phenyl ring of the phenethyl sidearm (Cu–C, 2.936(4) Å, see Fig. 2 and Supplementary Fig. 1).

To get insights into the ligand effect on the structure of copper (II) oxidation state, a copper(II)-chloride complex of L^{Pym} was also prepared by treating an equimolar amount of the ligand and Cu^{II}Cl$_2$ in CH$_3$CN (see Supplementary Methods). Single crystals of the copper(II)-chloride complex suitable for X-ray crystallographic analysis were obtained as a BF$_4^-$ salt, [Cu^{II}(L^{Pym})(Cl)] (BF$_4$), by treating the generated copper(II)-chloride complex with NaBF$_4$ (Supplementary Fig. 2 and Supplementary Tables 1 and 2). The copper(II) complex shows a square pyramidal structure, where the basal plane is occupied by the three nitrogen atoms of the ligand, N(1), N(2), and N(3), and the chloride counter anion, Cl(1), and the axial position is weakly coordinated by another chloride anion, Cl(2), of a neighboring copper(II) complex (Supplementary Fig. 2). Apparently, the square pyramidal structure of the copper(II) complex of L^{Pym} is different from that of the copper(II) complex of L^{Pye}, [Cu^{II}(L^{Pye})(Cl)]$^+$, which exhibits a tetrahedrally distorted four-coordinate structure as reported in our previous paper.[23]

In a cyclic voltammetric (CV) measurement, the copper(I) complex of L^{Pym} exhibits a quasi-reversible Cu^I/Cu^{II} redox couple at 0.17 V vs SCE in acetone, which is negative as compared to that of the copper(I) complex of L^{Pye} (0.40 V, see Supplementary Fig. 3). The result clearly indicates that electron donating ability of L^{Pym} is higher than that of L^{Pye}.
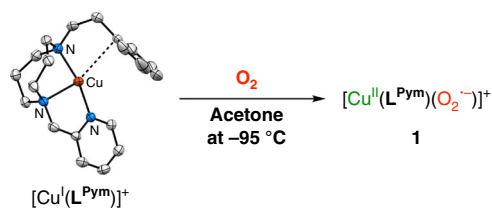

Fig. 1 Structures of tridentate ligands L^{Pym} and L^{Pye}. L^{Pym} 1-phenethyl-5-(pyridin-2-ylmethyl)-1,5-diazocane. L^{Pye} 1-phenethyl-5-[2-(pyridin-2-yl)ethyl]-1,5-diazocane

Fig. 2 Generation of copper(II)-superoxide complex 1. The reaction of [Cu^I(L^{Pym})]$^+$ (0.10 mM) with O$_2$ gas was conducted in acetone at –95 °C

Copper(I)-O$_2$ reactivity. Treatment of the copper(I) complex [Cu^I(L^{Pym})](BPh$_4$) (0.10 mM) with dry O$_2$ gas in acetone at a low temperature (−95 °C) resulted in a spectral change, where an intense LMCT band at 386 nm (ε = 4430 M^{-1} cm^{-1}) appeared together with broad bands at 558 nm (ε = 820) and 725 nm (ε = 1,160) as shown in Fig. 3 (red spectrum).[27] The spectrum is similar to that of the mononuclear copper(II)-(end-on)-superoxide complex **2** generated by using L^{Pye},[14,23] indicating the formation of a similar end-on superoxide copper(II) complex **1** (Fig. 2). In fact, the oxygenated product showed isotope-sensitive resonance Raman bands at 1064 and 464 cm^{-1}, which shifted to 997 cm^{-1} ($\Delta\nu_{O(16)-O(18)}$ = 67 cm^{-1}) and 451 cm^{-1} ($\Delta\nu_{O(16)-O(18)}$ = 13 cm^{-1}), respectively, upon using ^{18}O$_2$ instead of ^{16}O$_2$ (Supplementary Fig. 4a). Although interpretation is somewhat complicated by the presence of solvent peaks, the peak positions as well as the observed isotope shifts are similar to those of the O–O and the Cu–O stretching vibrations of the reported mononuclear copper(II)-(end-on)superoxide complexes.[10] Furthermore, the Cu:O$_2$ = 1:1 stoichiometry was confirmed by the titration of oxygenated product with ferrocene carboxylic acid (Supplementary Fig. 4b, c),[28] which confirmed the formation of mononuclear copper-dioxygen adduct complex.
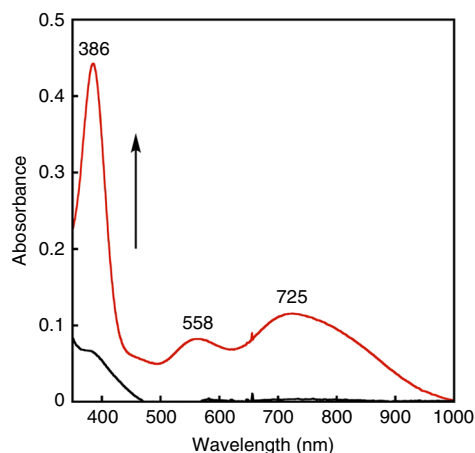

Fig. 3 UV–vis spectrum of superoxide complex **1**. UV–vis spectrum of copper(II)-(end-on)superoxide complex **1** (red line) obtained upon the treatment of [Cu^I(**L^{Pym}**)](BPh$_4$) (0.10 mM, black) with dry O$_2$ gas in acetone at −95 °C

Reactivity of copper(II)-superoxide complexes. Superoxide complex **1** gradually decomposed at a higher temperature (−60 °C; Supplementary Fig. 5a). In contrast to superoxide complex **2** supported by L^{Pye}, however, no aliphatic ligand hydroxylation took place after the reaction; **2** has been demonstrated to induce benzylic ligand hydroxylation of the phenethyl sidearm.[14] The decay of **1** obeyed first-order kinetics (Supplementary Fig. 5b), and the first-order kinetics was further confirmed by the fact that rate constants (k_{obs}) of the decay were virtually independent on the initial concentrations of **1** (0.10–0.50 mM) as shown in Supplementary Fig. 5c. These results confirm that the decay of **1** is a uni-molecular process with respect to the copper complex, and involvement of a dinuclear copper species such as a (μ-peroxido)dicopper(II) or a bis(μ-oxido)dicopper(III) complex or possibility of disproportionation of **1** during the decay process can be ruled out.

To our surprise, detailed product analysis of the final reaction mixture (work-upped at room temperature) indicated the formation of the aldol product (4-hydroxy-4-methylpentan-2-one; (CH$_3$)$_2$C(OH)CH$_2$C(O)CH$_3$) derived from two molecules of acetone (solvent) in a 560% based on **1**. Thus, this is a catalytic C–C bond formation reaction of the carbonyl compounds. Such an aldol-type reaction of acetone did not proceed at all in the case of superoxide complex **2**. To get insights into the reaction mechanism, we then examined the reaction of **1** and a series of carbonyl compounds in acetone.

First, the reaction of **1** with benzaldehyde (**3a**, C$_6$H$_5$CHO) was examined (Fig. 4). Treatment of **1** (0.10 mM) with an excess amount **3a** (1.0 mM) in acetone caused a significant increase in the decay rate of **1** even at a low temperature (−95 °C) as shown in Fig. 4a. The reaction also obeyed first-order kinetics (Fig. 4b), and the decay rates showed the first-order dependence on the benzaldehyde concentration, giving a second-order rate constant as 2.1 ± 0.2 M^{-1} s^{-1} (Supplementary Fig. 11). Then, the substituent effects of the substrate were examined using a series of p-substituted benzaldehyde derivatives (p-X-C$_6$H$_4$CHO; X = H: **3a**, X = NO$_2$: **3b**, X = Br: **3c**, X = Cl: **3d**, X = CH$_3$: **3e**, and X = OCH$_3$: **3f**, Supplementary Figs. 6–10). As clearly seen in Fig. 4c, the second-order rate constants increase as the electron-withdrawing ability of the p-substituent increases to give a positive Hammett ρ value as 2.2 (R = 0.98). The result clearly demonstrates a nucleophilic reactivity of superoxide complex **1** toward benzaldehyde derivatives. On the other hand, superoxide complex **2** did not react with these benzaldehyde derivatives under the same experimental conditions. The nucleophilic reactivity of **1** was more prominent in the reaction with ketones.
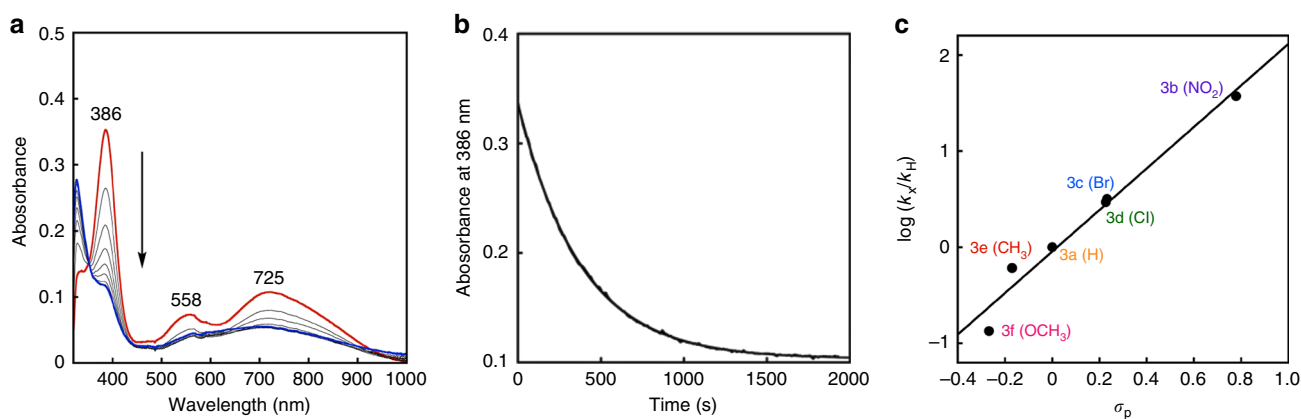

Fig. 4 Kinetic analysis on the reaction of **1** and benzaldehyde derivatives. **a** UV–vis spectral change in the reaction of **1** (0.10 mM) with benzaldehyde (**3a**, 1.0 mM) in acetone at −95 °C. **b** The time course of the decay at 386 nm. **c** Hammett plot for the reaction of **1** with p-substituted benzaldehydes (**3a-3f**) in acetone at −95 °C

Namely, **1** did not react with acetophenone (C₆H₅C(O)CH₃), whereas it did react with 2,2,2-trifluoroacetophenone (C₆H₅C(O)CF₃, **3j**) to provide a similar spectral change as shown in Supplementary Fig. 12 (the second-order rate constant was 7.9 ± 0.4 M⁻¹ s⁻¹). Nucleophilic and electrophilic reactivity of a nickel (II)-superoxide was recently reported.[29]

The intermediate generated in the reaction of **1** and **3a** at the low temperature (blue spectrum in Fig. 4a) may be a superoxide adduct of benzaldehyde **IM1** (detailed reaction mechanism is discussed below, Fig. 6). In fact, almost no kinetic deuterium isotope effect was observed, when deuterated benzaldehyde-d_1 (C₆H₅CDO) was employed ($k_H/k_D = 0.98 \pm 0.08$) (Supplementary Fig. 13). Formation of the copper(II)-alkylperoxido-type intermediate (**IM1**) was also supported by the resonance Raman spectrum shown in Supplementary Fig. 14. The intermediate showed isotope-sensitive resonance Raman bands at 876 and 508 cm⁻¹, which shifted to 852 cm⁻¹ ($\Delta\nu_{O(16)-O(18)} = 24$ cm⁻¹) and 490 cm⁻¹ ($\Delta\nu_{O(16)-O(18)} = 18$ cm⁻¹), respectively, upon ¹⁸O-substitution. The peak positions as well as the observed isotope shifts are similar to those of the O–O and Cu–O stretching vibrations of the reported mononuclear copper(II)-alkylperoxide complexes.[10]

Catalytic C–C bond formation reaction. The reaction of benzaldehyde **3a** was examined in a preparative scale (Table 1). Treatment of **3a** (25 μmol) with a catalytic amount of [Cuᴵ(**L**ᴾʸᵐ)](BPh₄) (10 mol%) in acetone (2.0 mL) under O₂ at 30 °C for 5 h gave 4-hydroxy-4-phenyl butanone (**4a**) in a 74% yield (Entry 1) based on **3a**; thus, turnover number of the copper complex was 7.4. Copper(I) complex [Cuᴵ(**L**ᴾʸᵐ)](PF₆) gave a comparable yield (61%) to that of [Cuᴵ(**L**ᴾʸᵐ)](BPh₄) (Entry 2). On the other hand, no reaction (NR) took place in the absence of **1** or under anaerobic conditions (Entries 3 and 4). KO₂ itself was not effective, suggesting that free superoxide anion is not an active species (Entry 5). Neither copper(I) complex supported by **L**ᴾʸᵉ nor the copper(II) complex of **L**ᴾʸᵐ was sufficient catalyst (Entries 6 and 7). These results unambiguously demonstrate that superoxide complex **1** is essential for the catalytic C–C bond formation reaction, and that simple Lewis acid catalysis by the copper(I/II) complexes can be ruled out.

The aldol products (**4a**–**4f**) were obtained in the reaction with the series of benzaldehyde derivatives (**3a**–**3f**, Fig. 5), where higher yields were obtained with the substrates having stronger electron-withdrawing *p*-substituent (**3b**–**3d**; X = NO₂, Br, Cl). The results are consistent with the kinetic data shown in Fig. 4c.

4a (X = H) 74%
4b (X = NO₂) >99%
4c (X = Br) 93%
4d (X = Cl) 93%
4e (X = CH₃) 51%
4f (X = OCH₃) 18%

4g 75%
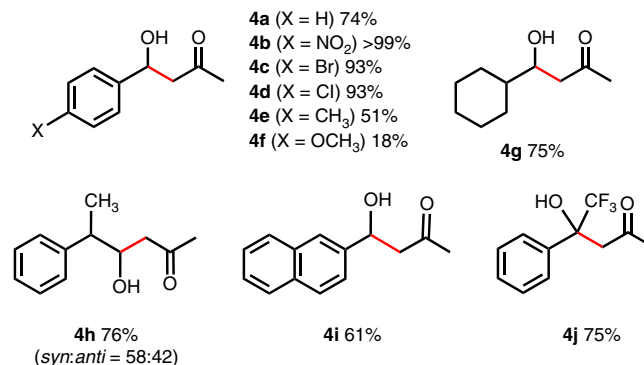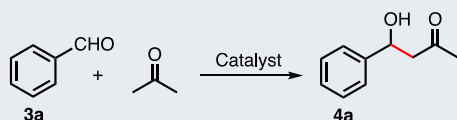
4h 76% (*syn*:*anti* = 58:42)

4i 61%

4j 75%

Fig. 5 Catalytic C–C bond formation in the reaction of **1** with aldehydes or ketone. Reaction conditions: substrate (25 μmol), catalyst (2.5 μmol), in acetone (2.0 mL) under O₂ (1 atm) at 30 °C for 5 h. The yields of products were determined by ¹H NMR based on substrates (carbonyl compounds) using 1,1,2,2-tetrachloroethane as an internal standard

where the rate constant increases with increasing the electron-withdrawing ability of the *p*-substituents. The catalytic reaction can be adapted to other aldehydes such as cyclohexanecarbaldehyde (**3g**, CCA), 2-phenylpropionaldehyde (**3h**, 2-PPA), and 2-naphtaldehyde (**3i**) to give the corresponding aldol products **4g**, **4h**, and **4i** in 75%, 76%, and 61%, respectively. Product **4h** was in a little favor of the *syn* product (*syn*: *anti* = 58:42). In these reactions, the oxidative deformylation products were not obtained from the final reaction mixture. Ketone with electron-withdrawing group such as 2,2,2-trifluoroacetophenone (**3j**) also gave the corresponding aldol product **4j** in a 75% yield, which is also consistent with the kinetic result (Supplementary Fig. 12).

Computational study. DFT calculations have been carried out to get detailed insights into the reaction mechanism of the catalytic C–C bond formation reaction (Fig. 6). As experimentally observed, superoxide complex **1** attacks the carbonyl carbon of benzaldehyde to give an alkylperoxido/alkoxyl radical intermediate (**IM1**). The DFT calculation suggests that association of an acetone molecule to the cupric ion stabilizes the intermediate **IM1** by 6.0 kcal mol⁻¹ (Supplementary Fig. 15). Existence of the copper(II)-alkylperoxido substructure in **IM1** was also confirmed by the resonance Raman spectra as described above (Supplementary Fig. 14). Furthermore, the DFT results indicated that **IM1**ˣ (X = NO₂, Cl, H, CH₃, OCH₃) generated by the reaction of complex **1** with a series of *p*-substituted benzaldehyde derivatives (**3a**, **3b**, **3d**, **3e**, and **3f**) becomes more stable as the electron-withdrawing ability of the *p*-substituent increases (Supplementary Fig. 16). This computational result is completely consistent with the experimental results (Hammett analysis) shown in Fig. 4c.

In the next step, we found two types of transition states (**TS1**ˢ and **TS1**ᴾ) for the hydrogen migration process from the associated acetone molecule. **TS1**ˢ is a transition state, in which a proton (H⁺) transfer from the acetone molecule to the benzylic oxygen O(4) takes place with an activation barrier of 7.3 kcal mol⁻¹, where a superoxido-type canonical form is dominant (O(1)–O(2):1.29 Å; spin density: O(1) = 0.60, O(2) = 0.46) with an alkoxide character on O(4) (spin density: 0.00). Another transition state **TS1**ᴾ is consisting of a peroxido-type canonical form (O(1)–O(2):1.44 Å; spin density: O(1) = 0.14, O(2) = 0.00) with an alkoxyl radical character on O(4) (spin density: 0.55), which induces hydrogen atom (H•) transfer with an activation barrier of 14.4 kcal mol⁻¹. Therefore, the intramolecular electron transfer from the peroxido moiety O(1)–O(2) to the alkoxyl radical group O(4) in **IM1** takes place to increase the basicity of

Table 1 Formation of 4-hydroxy-4-phenyl butanone (4a) in the reaction of benzaldehyde (3a) in acetone

Entry	Catalyst	Yield of 4a (%)
1	[Cuᴵ(**L**ᴾʸᵐ)](BPh₄)	74
2	[Cuᴵ(**L**ᴾʸᵐ)](PF₆)	61
3	None	NR
4ᵃ	[Cuᴵ(**L**ᴾʸᵐ)](BPh₄)	NR
5	KO₂	<1
6	[Cuᴵ(**L**ᴾʸᵉ)](PF₆)	<1
7	[Cuᴵᴵ(**L**ᴾʸᵐ)](OTf)₂	NR

Reaction conditions: **3a** (25 μmol), catalyst (2.5 μmol), in acetone (2.0 mL) under O₂ (1 atm) at 30 °C for 5 h. The yields of **4a** were determined by ¹H NMR based on benzaldehyde using 1,1,2,2-tetrachloroethane as an internal standard. ᵃ Under N₂
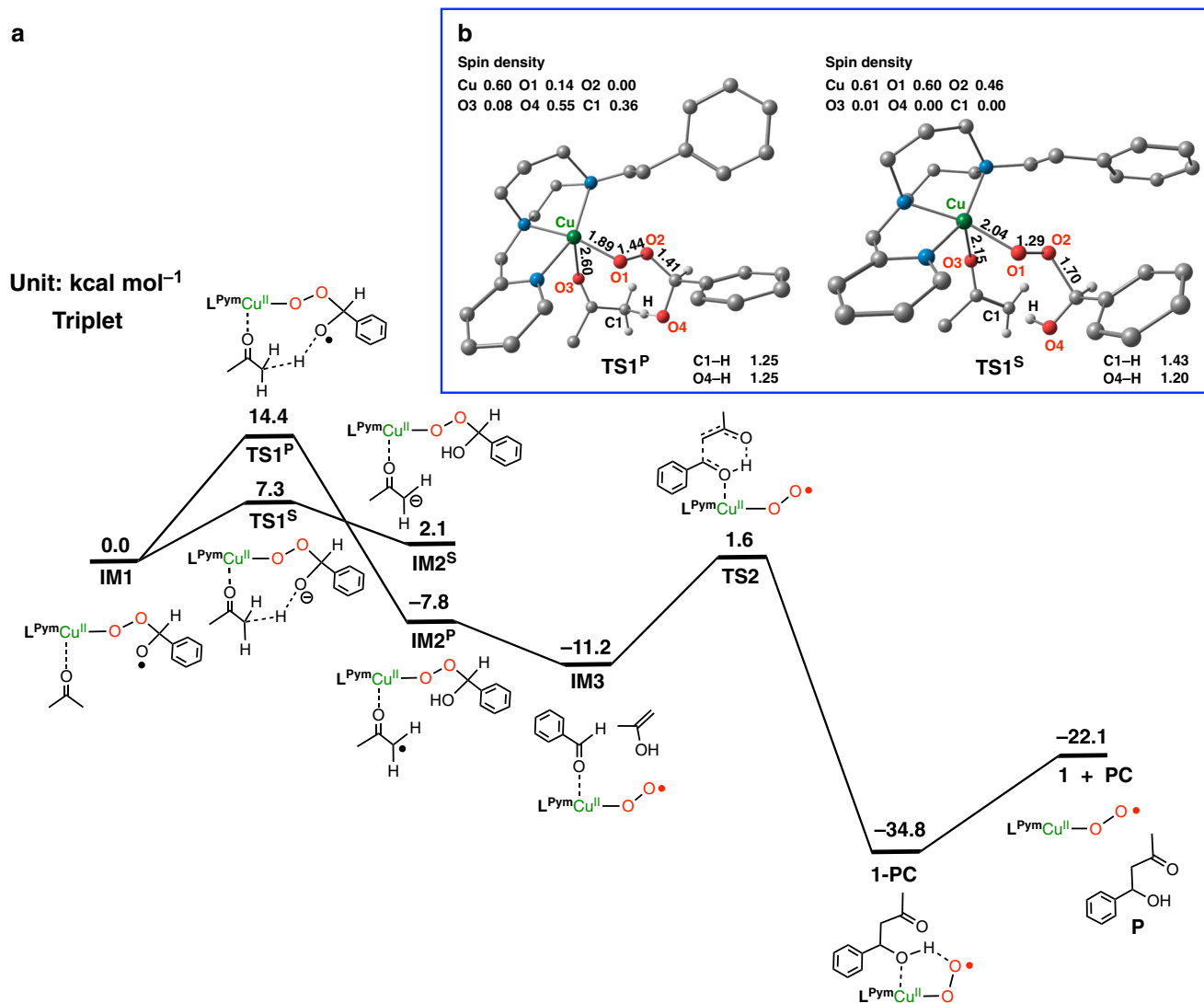
Fig. 6 Energy profile for the C–C bond formation by the reaction of **1** with benzaldehyde. **a** The relative energies with respect to **IM1** in the triplet ground state are in kcal mol^{-1}. **b** The transition state structures of **TS1^P** and **TS1^S** are shown together with their representative bond lengths (Å) and spin density

benzylic oxygen O(4), which enable to induce the proton (H$^+$) abstraction from the acetone molecule. After this step, the generated superoxido-type intermediate **IM2^S** having a shorter O (1)–O(2) bond (1.30 Å) with an anionic character on C(1) (spin density: 0.01) returns to the peroxido-type intermediate **IM2^P** with a longer O(1)–O(2) bond (1.43 Å) with a radical character on C(1) (spin density: 0.81), since the latter is more stable compared to the former by 9.9 kcal mol^{-1} (Fig. 6; Supplementary Fig. 17). Then, **IM2^P** is converted to a superoxide complex with the enolate of acetone (**IM3**), which is more stable compared to **IM2^P** by 3.4 kcal mol^{-1}. We examined the proton transfer process from **IM1** to **IM3** kinetically at –65 °C to obtain apparent kinetic deuterium isotope effect k^H/k^D as 2.7 by using acetone-d_6 as the solvent ($k^H = 5.6 \times 10^{-3}$ s^{-1} for acetone-h_6 and $k^D = 2.1 \times 10^{-3}$ s^{-1} for acetone-d_6, see Supplementary Fig. 18). Such a relatively small KIE value (2.7) may be consistent with the proton (H$^+$) transfer rather than hydrogen atom (H•) transfer. An analogous mechanism involving keto–enol tautomerization has been recently reported for the manganese(III)-peroxo catalyzed deformylation of aldehydes.[30,31] Then, C–C bond formation takes place through **TS2** to provide the product

1-PC with an activation barrier of 12.8 kcal mol^{-1}, completing the catalytic cycle.

Discussion

In this study, we have found that the mononuclear copper(II)-(end-on)superoxide complex **1** supported by a simple tridentate ligand **L^{Pym}** shows an unprecedented, to our knowledge, reactivity toward carbonyl compounds (substrate) to induce catalytic C–C bond formation with the solvent molecule (acetone), giving an β-hydroxy-ketones (aldol). Based on the detailed kinetic and DFT studies, we suggest that the superoxide complex exhibits nucleophilic reactivity toward carbonyl compounds to give the copper(II)-alkylperoxido/alkoxyl radical intermediate **IM1**, from which keto–enol tautomerization of the solvent molecule takes place via proton transfer through **TS1^S** and subsequent C–O bond homolysis giving **IM3**, regenerating the superoxide species. Then, the generated enol attacks the carbonyl group of substrates giving the aldol products (Fig. 6).

Such a catalytic C–C bond formation reaction did not occur at all, when the superoxide complex **2** supported by **L^{Pye}** was employed instead of complex **1** of ligand **L^{Pym}**. We have already

reported that the copper(II) complexes of L^{Pye} favor four-coordinate distorted tetrahedral geometry.[23,32] On the other hand, the copper(II) complex of L^{Pym} favors a five-coordinate square pyramidal geometry (Supplementary Fig. 2). Therefore, the association of acetone molecule to the copper(II) center may occur more easily in the L^{Pym} ligand system as compared to the L^{Pye} ligand system (Supplementary Fig. 15). This may be a reason for such a difference in the reactivity between **1** and **2**. To examine this interpretation, we also performed DFT calculation on the reaction of copper(II)-superoxide complex **2** with benzaldehyde (Supplementary Fig. 19). Apparently, the energy gap between **2** and **IM1′** in the L^{Pye} ligand system is larger than that between **1** and **IM1** in the L^{Pym} ligand system (16.2 kcal mol^{-1} for L^{Pye} and 12.3 kcal mol^{-1} for L^{Pym}, see Supplementary Fig. 19a and Fig. 6). Moreover, the distance between the copper(II) ion and the oxygen atom of acetone in **IM1′** (L^{Pye}) is significantly longer (3.15 Å; Supplementary Fig. 19b) as compared to that in **IM1** (L^{Pym}) (2.34 Å; Supplementary Fig. 20a). Taken together, these preliminary computational results are consistent with our interpretation regarding to the ligand effects (L^{Pym} vs L^{Pye}) on the reactivity.

So far, copper/O$_2$ systems have been frequently employed in the oxidative C–C bond formation reactions in synthetic organic chemistry.[33] In most cases, the copper ion is simply considered as an electron transfer catalyst from a reduced transition metal catalyst to O$_2$, regenerating a reactive catalyst in a higher oxidation state or a simple Lewis acid catalyst to enhance the reactivity of the carbonyl compounds.[26] However, the present results suggest that there may be an alternative catalytic role of transition metal superoxide species in such C–C bond formation reactions.

Methods

Synthetic procedures. See Supplementary Methods.

X-ray structure determination. See Supplementary Figs. 1 and 2, Supplementary Tables 1 and 2, and Supplementary Data 1.

Electrochemical measurements. See Supplementary Fig. 3.

Resonance Raman measurements. See Supplementary Figs. 4a and 14.

Kinetic measurements. See Supplementary Figs. 4b, 4c, 5–13 and 18.

Computational methods. See Supplementary Figs. 15–17 and 19–25, and Supplementary Data 2.

General procedure for the catalytic C–C bond formation reactions. In a vial (4.0 mL), a copper complex (2.5 μmol) was dissolved in acetone (2.0 mL), and substrate (25 μmol) was added to the solution under N$_2$ atmosphere. Then, O$_2$ was bubbled to the solution and an O$_2$ balloon (1 atm) was attached at top of the vial. After the reaction, the solvent was removed under reduced pressure, and the products were confirmed by comparing their ^{1}H NMR spectra to those of the authentic samples (see Supplementary Methods). The product yields were determined by ^{1}H NMR using 1,1,2,2-tetrachloroethane (δ 5.97) as an internal standard.

Data availability

References

1. Que, L. & Tolman, W. B. Biologically inspired oxidation catalysis. *Nature* **455**, 333–340 (2008).
2. Tolman, W. B. & Solomon, E. I. Preface: forum on dioxygen activation and reduction. *Inorg. Chem.* **49**, 3555–3556 (2010).
3. van der Donk, W. A., Krebs, C. & Bollinger, J. M. Jr. Substrate activation by iron superoxo intermediates. *Curr. Opin. Struct. Biol.* **20**, 673–683 (2010).
4. Ray, K., Pfaff, F. F., Wang, B. & Nam, W. Status of reactive non-heme metal–oxygen intermediates in chemical and enzymatic reactions. *J. Am. Chem. Soc.* **136**, 13942–13958 (2014).
5. Nam, W. Synthetic mononuclear nonheme iron–oxygen intermediates. *Acc. Chem. Res.* **48**, 2415–2423 (2015).
6. Sahu, S. & Goldberg, D. P. Activation of dioxygen by iron and manganese complexes: a heme and nonheme perspective. *J. Am. Chem. Soc.* **138**, 11410–11428 (2016).
7. Peck, S. C. & van der Donk, W. A. Go it alone: four-electron oxidations by mononuclear non-heme iron enzymes. *J. Biol. Inorg. Chem.* **22**, 381–394 (2017).
8. Fiedler, A. T. & Fischer, A. A. Oxygen activation by mononuclear Mn, Co, and Ni centers in biology and synthetic complexes. *J. Biol. Inorg. Chem.* **22**, 407–424 (2017).
9. Itoh, S. Mononuclear copper active-oxygen complexes. *Curr. Opin. Chem. Biol.* **10**, 115–122 (2006).
10. Elwell, C. E. et al. Copper–oxygen complexes revisited: structures, spectroscopy, and reactivity. *Chem. Rev.* **117**, 2059–2107 (2017).
11. Quist, D. A., Diaz, D. E., Liu, J. J. & Karlin, K. D. Activation of dioxygen by copper metalloproteins and insights from model complexes. *J. Biol. Inorg. Chem.* **22**, 253–288 (2017).
12. Würtele, C. et al. Crystallographic characterization of a synthetic 1:1 end-on copper dioxygen adduct complex. *Angew. Chem. Int. Ed.* **45**, 3867–3869 (2006).
13. Maiti, D. et al. A 1:1 Copper-dioxygen adduct is an end-on bound superoxo copper(II) complex which undergoes oxygenation reactions with phenols. *J. Am. Chem. Soc.* **129**, 264–265 (2007).
14. Kunishita, A. et al. Mononuclear copper(II)-superoxo complexes that mimic the structure and reactivity of the active centers of PHM and DβM. *J. Am. Chem. Soc.* **131**, 2788–2789 (2009).
15. Donoghue, P. J., Gupta, A. K., Boyce, D. W., Cramer, C. J. & Tolman, W. B. An anionic, tetragonal copper(II) superoxide complex. *J. Am. Chem. Soc.* **132**, 15869–15871 (2010).
16. Peterson, R. L. et al. Cupric superoxo-mediated intermolecular C-H activation chemistry. *J. Am. Chem. Soc.* **133**, 1702–1705 (2011).
17. Kobayashi, Y. et al. Copper(I)-dioxygen reactivity in a sterically demanding tripodal tetradentate tren ligand: formation and reactivity of a mononuclear copper(II) end-on superoxo complex. *Eur. J. Inorg. Chem.* **2012**, 4574–4578 (2012).
18. Lee, J. Y. et al. Mechanistic insights into the oxidation of substituted phenols via hydrogen atom abstraction by a cupric–superoxo complex. *J. Am. Chem. Soc.* **136**, 9925–9937 (2014).
19. Kim, S. et al. A N3S(thioether)-ligated cuII-superoxo with enhanced reactivity. *J. Am. Chem. Soc.* **137**, 2796–2799 (2015).
20. Fujisawa, K., Tanaka, M., Morooka, Y. & Kitajima, N. A monomeric side-on superoxocopper(II) complex: Cu(O$_2$)(HB(3-tBu-5-iPrpz)$_3$). *J. Am. Chem. Soc.* **116**, 12079–12080 (1994).
21. Sanchez-Eguia, B. N., Flores-Alamo, M., Orio, M. & Castillo, I. Side-on cupric-superoxo triplet complexes as competent agents for H-abstraction relevant to the active site of PHM. *Chem. Commun.* **51**, 11134–11137 (2015).
22. Iovan, D. A. et al. Reactivity of a stable copper-dioxygen complex. *Chem. Commun.* **53**, 10306–10309 (2017).
23. Kunishita, A. et al. Active site models for the CuA site of peptidylglycine α-Hydroxylating monooxygenase and dopamine β-monooxygenase. *Inorg. Chem.* **51**, 9465–9480 (2012).
24. Tano, T. et al. Redox properties of a mononuclear copper(II)-superoxide complex. *Inorg. Chem.* **52**, 10431–10437 (2013).
25. Pirovano, P. et al. Nucleophilic reactivity of a copper(II)–superoxide complex. *Angew. Chem., Int. Ed.* **53**, 5946–5950 (2014).
26. Allen, S. E., Walvoord, R. R., Padilla-Salinas, R. & Kozlowski, M. C. Aerobic copper-catalyzed organic reactions. *Chem. Rev.* **113**, 6234–6458 (2013).
27. Woertink, J. S. et al. Spectroscopic and computational studies of an end-on bound superoxo-Cu(II) complex: geometric and electronic factors that determine the ground state. *Inorg. Chem.* **49**, 9450–9459 (2010).
28. Herres-Pawlis, S. et al. Phenolate hydroxylation in a Bis(mu-oxo)dicopper(III) complex: lessons from the guanidine/amine series. *J. Am. Chem. Soc.* **131**, 1154–1169 (2009).
29. Panda, C. et al. Nucleophilic versus electrophilic reactivity of bioinspired superoxido nickel(II) complexes. *Angew. Chem., Int. Ed.* **57**, 14883–14887 (2018).

30. Prasenjit, B. et al. Deformylation reaction by a nonheme manganese (III)–peroxo complex via initial hydrogen-atom abstraction. *Angew. Chem., Int. Ed.* **55**, 11091–11095 (2016).

31. Cantú Reinhard, F. G. et al. Keto–enol tautomerization triggers an electrophilic aldehyde deformylation reaction by a nonheme manganese(III)-peroxo complex. *J. Am. Chem. Soc.* **139**, 18328–18338 (2017).

32. Abe, T. et al. Geometric control of nuclearity in copper(I)/dioxygen chemistry. *Inorg. Chem.* **53**, 8786–8794 (2014).

33. Evano, G., Blanchard, N. & Toumi, M. Copper-mediated coupling eactions and their applications in natural products and designed biomolecules synthesis. *Chem. Rev.* **108**, 3054–3131 (2008).

Author contributions

The manuscript was achieved through contributions of all authors. T.A. and S.I. designed the project, conducted the experiments, and wrote the manuscript. Y.H., Y.S., and K.Y. performed DFT calculations. T. Ohta and T. Ogura contributed to the measurements of resonance Raman spectra. Y.M. and H.S. contributed to discussions.

Additional information

Competing interests: The authors declare no competing interests.

Reprints and permission information is available online at http://npg.nature.com/reprintsandpermissions/

Publisher's note: Springer Nature remains neutral with regard to jurisdictional claims in published maps and institutional affiliations.